



Spatial Variability and Time Decay of Rock Mass Mechanical Parameters: A Landslide Study in the Dagushan Open-Pit Mine

Feiyue Liu^{1,2} · Tianhong Yang¹ · Jingren Zhou³ · Wenxue Deng¹ · Qinglei Yu¹ · Penghai Zhang¹ · Guanwen Cheng¹

Received: 1 July 2019 / Accepted: 31 March 2020 / Published online: 23 May 2020
 © Springer-Verlag GmbH Austria, part of Springer Nature 2020

Abstract

Mechanical parameters of rock mass in mining engineering feature the characteristics of spatial variability and time decay, and it plays an important role in the slope stability analysis. The mechanical behaviour of rock engineering in low in-situ stress condition is highly affected by the rock mass quality. In this paper, the distribution of geological strength index (GSI) was obtained by geostatistics-based methods to determine the spatial variability of mechanical parameters. Moreover, mechanical parameters of rock masses in open-pit mine are deteriorating continuously in the mining process. A damage model using microseism (MS) data was proposed to describe the time decay of mechanical parameters. Additionally, the dynamic programming method was used to search the rough critical slip surface and factor of safety considering the heterogeneous mechanical parameters. An example was further employed to demonstrate these proposed methods in the Dagushan open-pit mine. The results indicated that incorporation of spatial variability and time decay into mechanical parameters led to a fundamental change in the slope stability. Our study helps to provide detailed mechanical parameters, which contribute to a more reasonable explanation as well as provide governance measures for the rock landslides.

Keywords Mechanical parameters · Block model · Geostatistics · Microseism · Dynamic programming · Landslide

List of Symbols

J_v	Volumetric frequency of discontinuities	x_v, x_i, d_i, N	Estimation point, i th sampling point participating in the estimation, the distance from i th sampling point to the estimation point and exponent related the degree of variation
T	Ratio of fracture element in rough discrete fracture network (RDFN) model of jointed rock mass	m_i	Material constant in the Hoek–Brown method
		U, U_E, U_D, U_M	Total energy exercised by external forces on rock mass, dissipation energy and releasable strain energy, MS energy in a rock mass unit
		$E_{UD}, E_D, c_{UD}, c_D, \varphi_{UD}, \varphi_D; D$	Elastic modulus, cohesion and friction of undisturbed and damaged rock mass; damage variable
		E_{MS}, V_A	Source energy and apparent volume of MS event
		η	Seismic efficiency
		M, G	Seismic moment of MS event, stiffness of rock mass

✉ Tianhong Yang
 yangtianhong@mail.neu.edu.com

¹ Center of Rock Instability and Seismicity Research, School of Resources and Civil Engineering, Northeastern University, Shenyang 110819, Liaoning, People's Republic of China

² Department of Civil Engineering, McMaster University, Hamilton, ON L8S 4L7, Canada

³ State Key Laboratory of Hydraulics and Mountain River Engineering, College of Water Resource and Hydropower, Sichuan University, Chengdu 610065, Sichuan, People's Republic of China

f_s	Factor of safety
τ_f, τ	Shear stress and shear strength
R_i, S_i	Actuating forces and resisting forces
$G_m, H_i(j)$	Auxiliary function and optimal function
$[i], \{j\}$	Stage and state point in the dynamic programming method
P, Q	Number of stage and state point
$\sigma_1, \sigma_2, \sigma_3$	Maximum, medium, and minimum principal stress in 3D space
$\sigma_x, \sigma_y, \tau_{xy}$	Horizontal stress, vertical stress and shear stress in 2D space

1 Introduction

Reliable estimates of rock mass properties are essential for almost any rock engineering. The quality of the geological models and of the geotechnical information available cannot be overemphasized. Without reliable background information, the rock engineering stability analysis becomes a meaningless exercise (Hoek 2007). The key to geotechnical numerical simulation is a rigorous mechanical model and precise mechanical parameters, and the results produced by numerical models are only as good as the input data. An accurate geological model is essential, and realistic estimates of heterogeneous rock mass mechanical parameters are required. Due to the inherent variability within natural geological structures, the rock mass properties have an obvious spatial variability even under the same lithology.

Ideally, enough natural geological data will give a detailed description of the spatial variability of rock mass properties, but expensive drilling costs limit the amount of geological data. Geotechnical design projects often suffer from inherent information deficiencies associated with the difficult and often impractical nature of collecting large datasets (Read and Stacey 2018). Fortunately, many geological parameters follow the geostatistics law that has an inner relationship with the spatial location (Caers 2005; Priest 1993; Rendu 1978). Stavropoulou et al. (2007) developed a quick solver in Fortran to perform variography analysis of 3D spatial data, and fast kriging estimation of RMR between borehole sampling locations. Mayer and Stead (Mayer and Stead 2017) compared the traditional, step-path, and geo-statistical methods in the stability analysis of the Ok Tedi large open-pit mine. The results indicated that oversimplification of the spatial heterogeneity favors conservative design practices,

with an overestimation of the probability of failure. Egaña and Ortiz (2013) presented the advantages of applying geostatistics in the assessment of geotechnical variables. In addition, many researchers have provided risk assessment in geotechnical engineering without natural geological data (Fenton and Griffiths 2008; Griffiths et al. 2009; Jiang et al. 2014; Li et al. 2015). Engineering experience indicates that at low in-situ stress conditions like slope engineering or low-buried tunnels, the failure of rock masses is often controlled by persistent natural discontinuities (Cai et al. 2001). In this paper, due to the landslide case study was an open-pit mine, we just focused on the spatial variability of rock mass quality GSI, other issues can be considered in the future work.

Furthermore, rock mass properties are time-dependent and loading-dependent. The deformability and strength characteristics of rock mass are inevitably reduced due to rock damage induced by excavation disturbances. Usually, a description of time decay rock mass behaviour should include the effect of mechanical parameters deteriorates with time and/or deformation. Related numerical methods are primarily focused on the strain-softening model (Bazant et al. 1984), rheology model (Cristescu and Hunsche 1998) and damage model (Tang 1997). By considering the continuum deterioration of mechanical parameters in the failure process, the strain-softening method can model the overall behaviour of rock mass without going into the micro-crack (Lee and Pietruszczak 2008; Wang et al. 2011). For the rheology model, the constitutive description for the time decay behaviour are based on the utilizing information obtained from rheology tests (Maranini and Yamaguchi 2001; Zhou et al. 2011), or the combination of several basic mechanical elements (Fakhimi and Fairhurst 1994; Malan 1999). The time decay of rock mass mechanical parameters is associated with the initiation, propagation, and coalescence of microcracks. Micromechanical damage models have been widely used to describe the time decay behaviour of rock mass (Zhu and Tang 2004). Besides, many researches indicated that the data-driven back analysis method is an effective tool to character time decay of rock mass (Feng et al. 2000; Sharifzadeh et al. 2013).

In recent years, the MS technique has been applied in various geotechnical engineering projects for daily safety monitoring (Lebert et al. 2011; Ma et al. 2015; Zhou et al. 2017). Many studies suggest that MS events are indicators of rock damage, and MS monitoring is an efficient method for observing rock damage. This nondestructive technique can achieve fast, accurate and real-time source location. The combination of numerical simulation and MS monitoring is a promising method for analysis of rock damage. The key issue is to establish a quantitative relationship between MS events and rock damage variables that modify the rock mass properties. Cai et al. (2001) proposed a softening anisotropic numerical model that used acoustic emission data as input to determine the state of

damage. Furthermore, Cai et al. (2007) presented a method to back-calculate the rock mass strength parameters using MS monitoring data. Xu et al. (2014) utilized the MS data as input to degrade the mechanical parameters of rock elements in the numerical model, and then recognized the potential sliding surface of the rock slope. Zhao et al. (2017) analysed the damage and failure characteristics of rock mass based on the analysis of the temporal and spatial change of MS events and source parameters. Zhou et al. (2018) proposed a numerical model coupling joints, water and microseismicity to simulate rock mass damage evolution process. In this paper, a MS-driven damage model based on energy dissipation theory was proposed to characterize the time decay of mechanical parameters.

A slope stability analysis consists of the determination of the critical slip surface with the lowest safety factor and the calculation of a safety factor for the specified critical slip surface. Classical limit equilibrium methods generally make use of assumptions regarding the relationship between the inter-slice forces. However, the actual stresses within a slope are quite irregular due to the heterogeneous mechanical parameters, which can lead to a more tortuous critical slip surface and an uncertain safety factor. By considering complex stress state and heterogeneous mechanical parameters, the dynamic programming method can provide a more complete solution for the slope stability analysis (Baker 1980; Pham and Fredlund 2003).

In this paper, we proposed a new approach for rock slope stability analysis considering both spatial variability and time decay mechanical parameters. As shown in Fig. 1, this method features the following main steps. First, the octree method was employed to discrete the research area into a block model. Then, specific geological data were collected, and spatial interpolation was used to ensure each block unit obtains its individual geological parameters with the geostatistical method. The spatial variability mechanical parameters in each block were obtained by the Hoek–Brown method (Hoek and Carranza-Torres 2002). Furthermore, a MS-driven damage model was established based on the energy dissipation theory. A program was developed with the FISH language embedded in FLAC to search rock units within the damage scope of MS events and weakening the mechanical parameter of rock units. The damage field evolution process was visualized, and a time decay mechanical parameters block model was obtained. At last, combined with the in-situ engineering investigation and heterogeneous mechanical parameters, a method combining dynamic programming and stress analysis was used to identify the potential tortuous critical slip surface and safety factor. As a case study, the Dagushan iron open-pit mine was employed to demonstrate the proposed approach.

2 Engineering Background

2.1 Project Overview

The Dagushan iron open-pit mine, located in Anshan City, Liaoning Province, P. R. China, was subject to the threat of landslide. As shown in Fig. 2a, the mine, with a length of 1620 m from east to west and a width of 1560 m from south to north, has been mined more than one hundred years and the depth has reached 450 m as of 2019. As shown in Fig. 2b, a research area was selected and a three-dimensional (3D) geological model shown in Fig. 2c has been built for the stability analysis. The research area contains four kinds of lithologies, including granite, phyllite, magnetite quartzite and porphyrite. In addition, there are two main faults on the left and right of the magnetite quartzite, namely, fault F14 and fault F15, respectively. The engineering geological investigation indicates that each fault has an average thickness of 6 m, and such information is presented in the 3D geological model.

As shown in Fig. 3a, a landslide with a height over 72 m occurred at the north of the open-pit on May 27, 2018. Actually, in the summer of 2017, a prediction was made for the location of landslide based on many premonitions, including large deformation and cracks on the slope surface of the open-pit (see Fig. 3b). A typical profile was selected to perform detailed slope stability analysis. As shown in Fig. 2c, the typical profile was located in the center of landslide zone and perpendicular to the slope surface. The direction of typical profile was 26.6° north to west. As shown in Fig. 2d, the engineering investigation presented the top and bottom border of the landslide in the typical profile. After the rock landslide, the local slope angle decreased from 47° to 42° . During the mining period from September 01, 2017 to May 27, 2018, two benches were excavated and the mining activities were mainly concentrated on the bottom border of the landslide. In addition, a detailed engineering geological investigation and a MS monitoring system were installed in the research area.

2.2 Laboratory Experiment

As shown in Fig. 4, cores with different types of lithologies were taken from the boreholes. During the cutting period, water was utilized to cool down the high temperature due to intense friction. Unfortunately, part of the specimen was inevitably injured for its fragile properties and water-weakening impact, especially rock samples from the fault zone and chlorites. The acoustic wave velocities of the specimens were investigated, and specimens with a large discreteness were excluded. Finally, more than 40

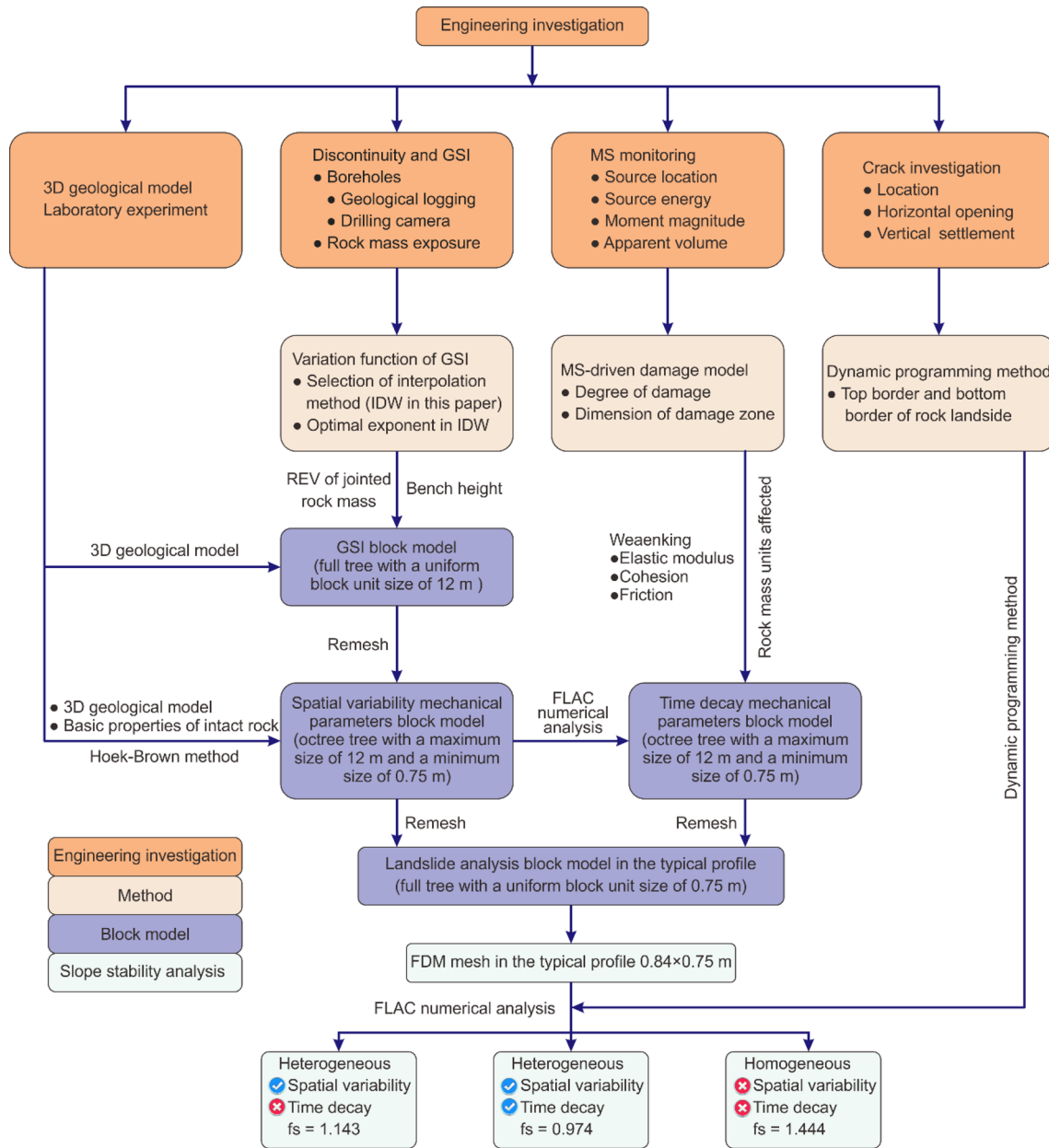


Fig. 1 Flowchart of the rock mass property modification

rock specimens were collected to test their basic physical and mechanical parameters.

In this paper, the Hoek–Brown method (Hoek and Carranza-Torres 2002) was used to evaluate the mechanical parameters of rock masses. The Hoek–Brown method started from the properties of intact rock and then introduced factors to reduce these properties on the basis of the characteristics of discontinuities in a rock mass, and it has been widely accepted and applied in a large number of rock projects around the world. According to the demands

of the Hoek–Brown method, the physical and mechanical properties of intact rock samples, including density, Poisson’s ratio and uniaxial compression strength (UCS) were measured. Density was measured with a high-precision equipment. Poisson’s ratio and UCS were measured using a compression testing machine. Besides, material constant (m_i) was assigned for each lithologies based on previously published literature (Hoek and Carranza-Torres 2002). The basic physical and mechanical parameters of the intact rock were listed in Table 1.

Fig. 2 Photograph of the Dagushan open-pit mine. **(a)** Overview of the Dagushan open-pit mine. **(b)** Overview of the study area. **(c)** 3D geological model of the study area. Migmatite in blue, porphyrite in green, magnetite quartzite in red, fault in yellow and chlorites in cyan-blue. Typical profile in gray, landslide zone in pink region, MS sensors in gray square (S9 for three-component MS sensor), boreholes in gray circle (ZK1 and ZK2 for geological logging, see Fig. 4; ZK3 for drilling camera measurement, see Fig. 5), photogrammetry measurements of rock exposure in gray band, and photogrammetry sampling point of Fig. 7 is located between MS sensor S1 and S2. **(d)** Rock landslide in the typical profile (color figure online)

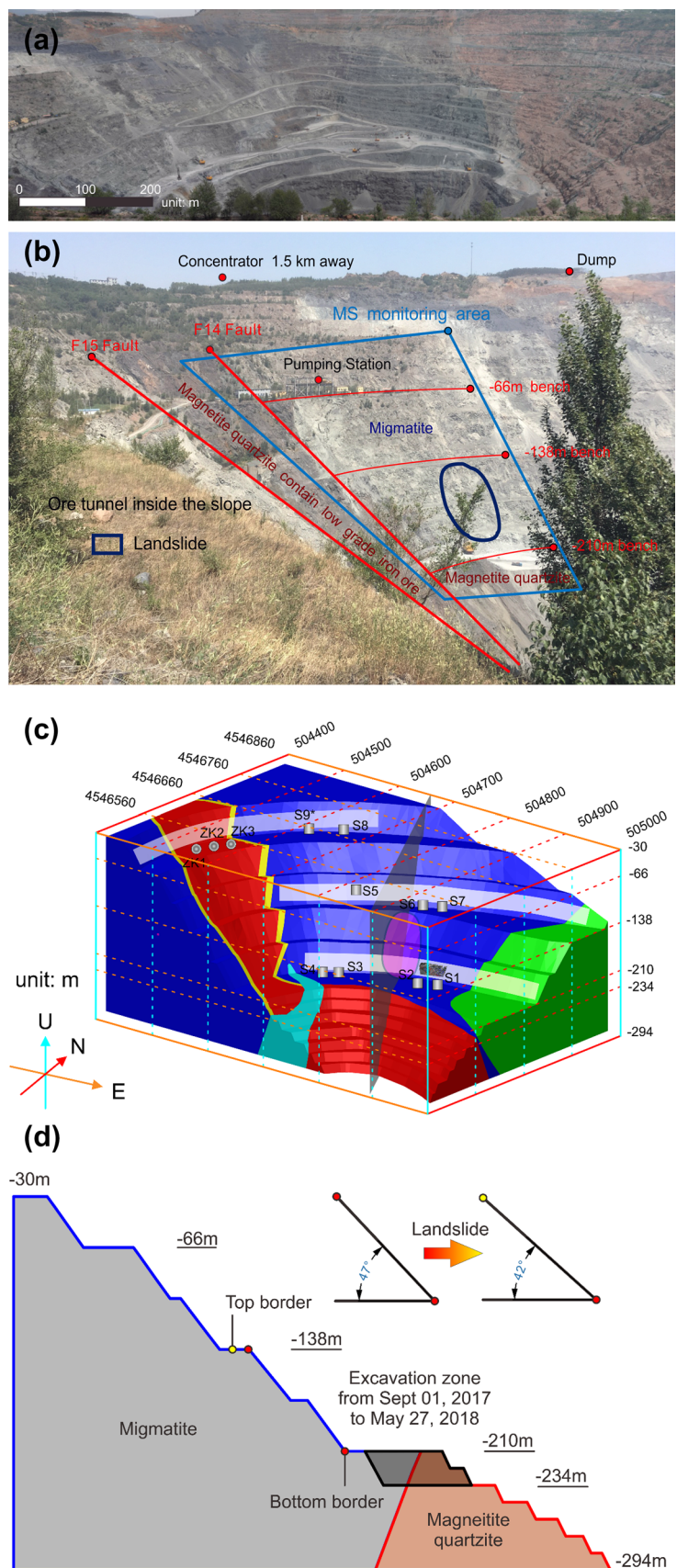
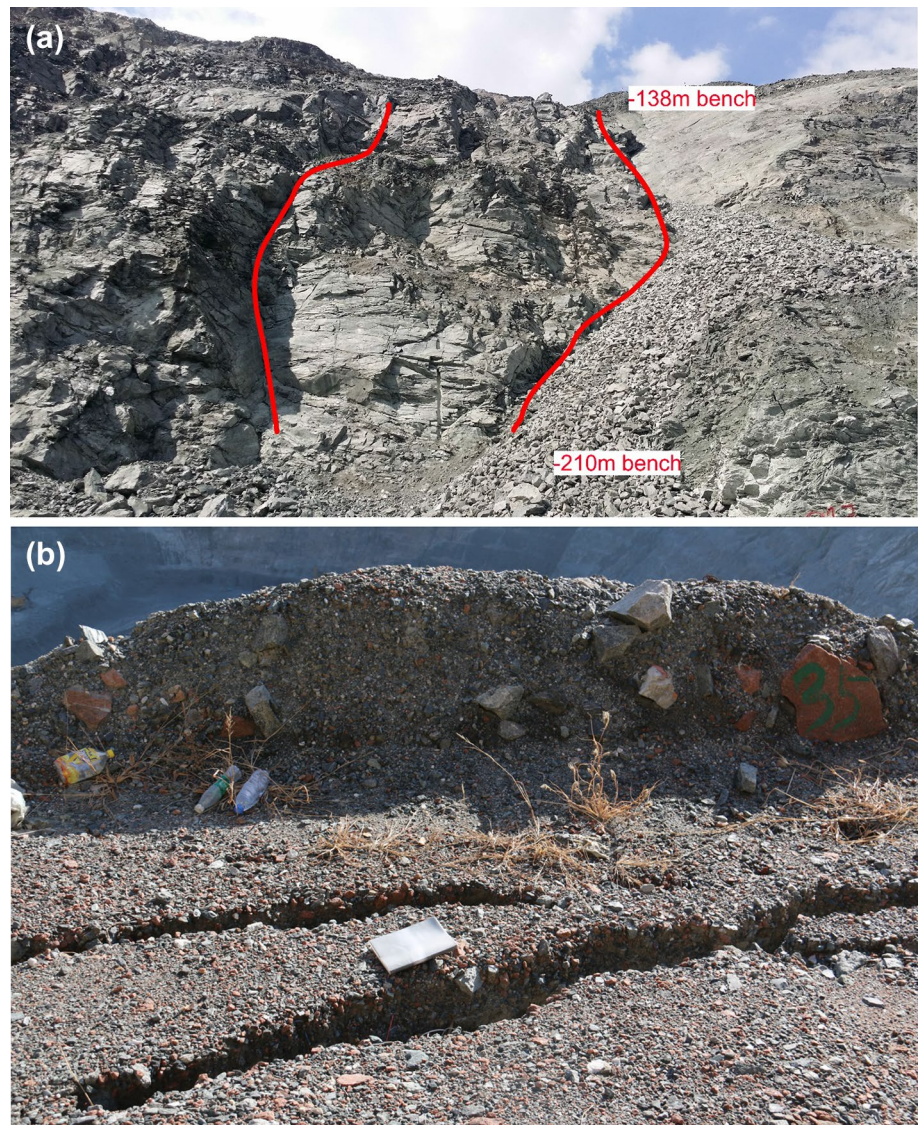


Fig. 3 Photograph of the rock mechanics disaster. **(a)** Photograph of landslides. Landslide border in red line. **(b)** Crack in the top border of landslide (– 138m bench) (color figure online)



2.3 Discontinuity and Rock Mass Quality

To adequately represent jointed rock mass in the 3D geological model, three methods were employed to obtain discontinuity data, including geological logging of typical boreholes (two boreholes including 16 sampling points, see Fig. 5), drilling camera measurements (one boreholes including 8 sampling points, see Fig. 6) and photogrammetry measurements of rock exposure (70 ShapeMetriX3D sampling points, see Fig. 7). Especially, the photogrammetry technique can get detailed discontinuity information from metric 3D images, including trace, trace length, volume frequency, dip angle and spacing. Such information was necessary for the size effect analysis of the jointed rock mass in Sect. 3.1.

In this paper, the GSI was used to quantify the rock mass quality. As shown in Fig. 8, the GSI can be obtained by two independent variables, namely the structure rating (SR)

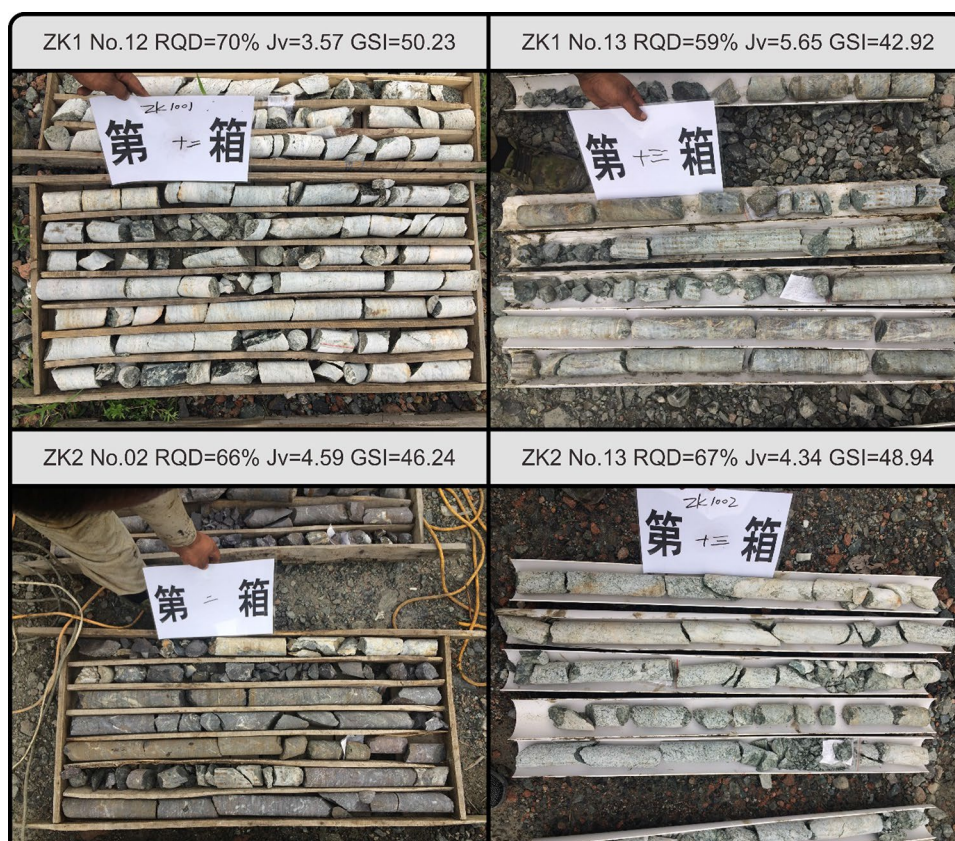
based on discontinuity volume frequency J_v , and the surface condition rating (SCR) based on the roughness (R_r), weathering (R_w) and infilling (R_f) of discontinuities. Those values can be found in Sonmez and Ulusay's (1999) previous study, and the SR and SCR can be obtained using the following expressions:

$$SR = -17.5 \ln J_v + 79.8, \quad (1)$$

$$SCR = R_r + R_w + R_f. \quad (2)$$

Finally, 94 discontinuity sampling points were placed in the research area, and each sampling point has its unique GSI value. Those sampling points are used to evaluate the spatial variability of rock mass quality GSI (see Sect. 4.1), and enough sampling points are needed in the

Fig. 5 Geological logging of typical borehole



accuracy of the MS monitoring system. As shown in Table 2, the average location error was 12.0 m.

The MS monitoring system in the Dagushan open-pit mine recorded signals from September 1, 2017 to December 31, 2017. During this period, the MS monitoring sensor array and distribution of MS events located in the study zone were presented in Fig. 9a. The events were coloured by moment magnitude and sized by source energy. The distribution of MS events in the typical profile was presented in Fig. 9b. The MS events' density in the landslide zone was much higher compared with the undisturbed area.

3 Octree-Based Block Model Generation

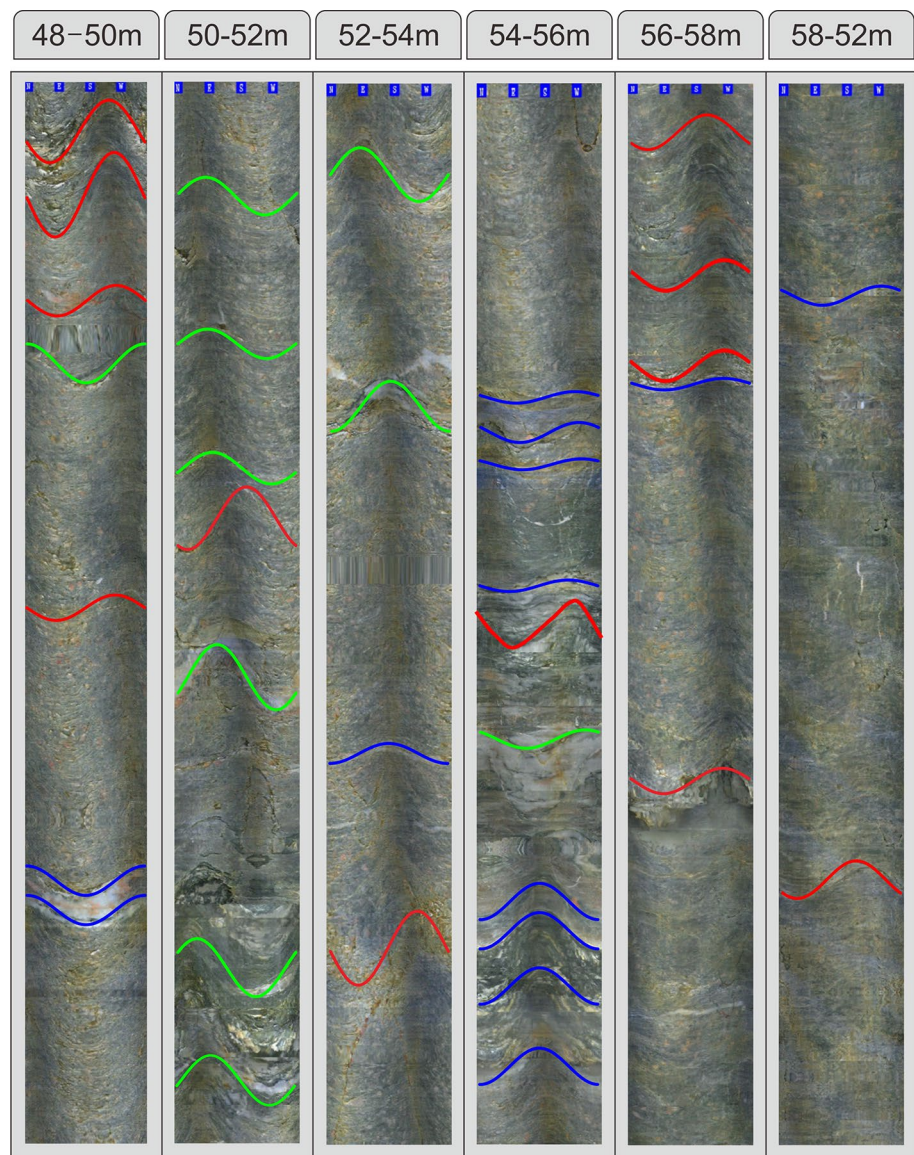
To describe the spatial distribution of rock mass properties via a block model, a large area rock mass should be divided into small units, and each unit should have distinct and definite parameters. The block model was used in this paper because it can meet the need of geostatistical analysis, i.e. each sample should have the same volume in the geostatistical analysis. The establishment of the block model simplifies the topology relationship, and reduces the computer memory usage, which assists in the implementation of this method. Furthermore, the block model can easily transform into a mesh of the finite difference method (FDM) if necessary.

Block-based methods have stood the test of time and have been implemented numerous in-situ engineering endeavours throughout the world (Caers 2005).

3.1 Size Effect of Jointed Rock Mass

The shape and size of the block units take an important role in the geostatistics-based estimation process and FDM analysis. Without loss of generality, we set the shape of the block units as cube, and the representative elementary volume (REV) of jointed rock mass was set as a reference value for the initial size of block units. As shown in Fig. 10a, the two-dimensional rough discrete fracture network (RDFN) models were generated with Fourier-based generic math method based on the discontinuity geometric information in Fig. 7. The digital image processing (DIP) technique was employed to analyse the size effect of jointed rock mass. First, a RDFN model was transformed to a picture with a definite rule. For example, the RDFN model with a size of 10 m was transformed into a picture (width: 1000 mm; height: 1000 mm; resolution: 300 dpi; line width of rough fracture: 1.5 mm; format: “.png”; background colour: white; fracture colour: black). Then, the picture was transferred to a matrix according to the greyscale, and the matrix can be divided into two parts: rock element and fracture

Fig. 6 Drilling camera measurements, $J_v=2.92$, $GSI=51.32$



element. Finally, the ratio of the fracture element in the matrix, T , was calculated.

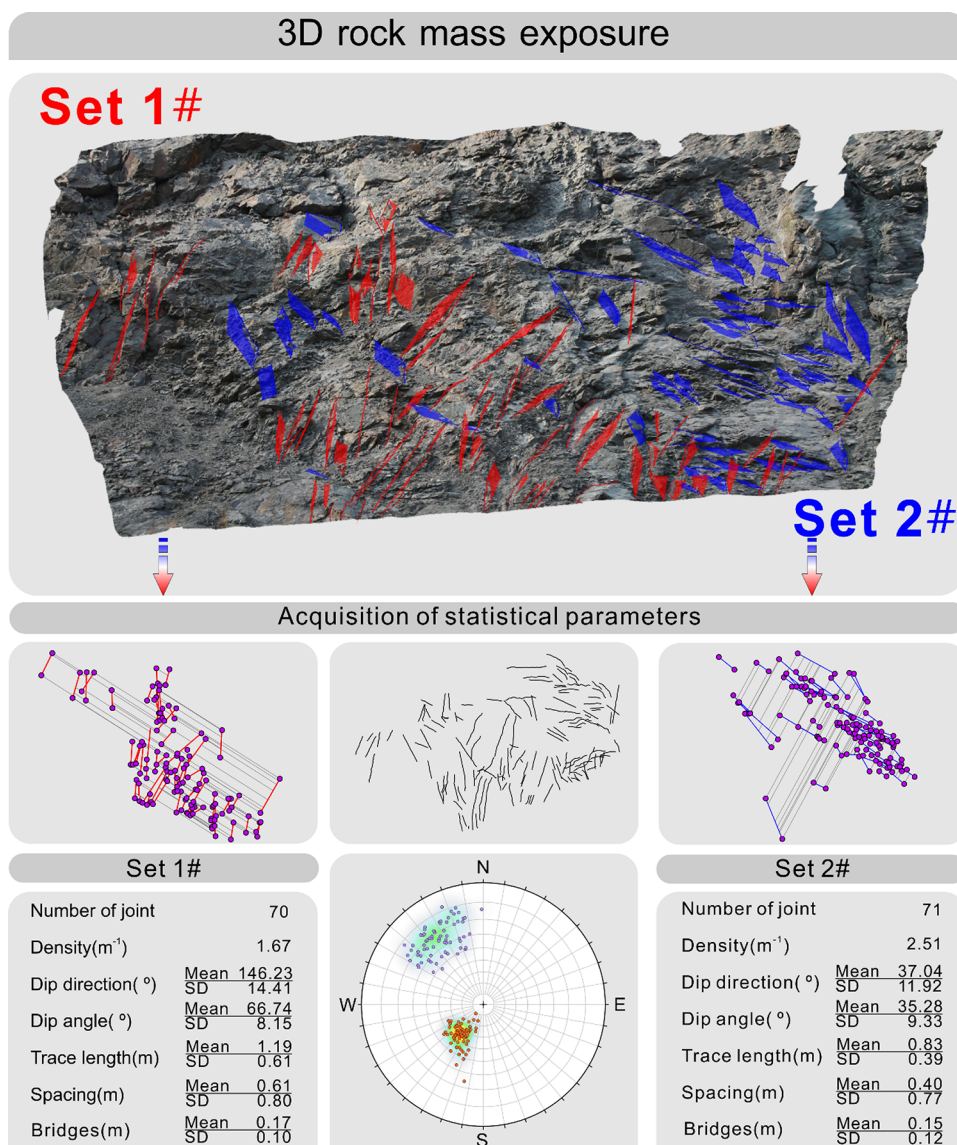
As shown in Fig. 10a, a series of RDFN models were performed to study the size effect of jointed rock mass. The relationship between the ratio of fracture element with the sample sizes is presented in Fig. 10b. The ratio of the fracture element was strongly affected by the sample size. The ratio was quite unstable when the sample size was less than 7 m, and the change of ratio was not significant when the sample size reached 8 m. The convergence condition was settled as Eq. (3) according to reference (Kanit et al. 2003), and these results indicate that the REV size for the jointed rock mass should be 10 m:

$$\frac{|T_{r+1}-T_r|}{T_r} \leq 1\%. \quad (3)$$

3.2 Generation of Block Model

In this paper, we combined all the geological information (GSI, lithology), physical and mechanical parameters for rock mass (density, wave velocity, elastic modulus, Poisson's ratio, compressive strength, tensile strength, cohesion and friction), mining information (mining schedule) in one block model. The octree-based block model generation method has been widely applied in the mining engineering, especially in the resource management and mining schedule of open-pit mines. The basic principle and coding process of the octree method can be found in the related literature (Yerry and Shephard 1984). As shown in Fig. 11, in this paper, three block models with different unit size were generated using the octree method:

Fig. 7 Photogrammetry measurements of rock exposure, $J_v=4.18$, $GSI=42.18$



1. A full tree with a uniform size of 12 m for the GSI block model (see Fig. 14). As mentioned before, the REV size for the jointed rock mass was 10 m, considering the bench height of the Dagushan open-pit mine was 12 m, to get a good compatibility with the 3D geological model, we adopt the 12 m as the unit size of the GSI block model.
2. An octree tree with a maximum size of 12 m and a minimum size of 0.75 m for the heterogeneous mechanical parameters block model (see Figs. 15, 17, 18). The mechanical parameters block model was then transformed into an FDM mesh for stress analysis. As we all know, a smaller mesh size will bring high-precision numerical simulation result. Also, smaller mesh size will increase the number of elements and the computing time. In the mechanical parameters block model, rock masses were remeshed in the region near to the slope surface, lithological interface and MS events. Due to the special demand of octree method, the mesh size must be the sequential half of the initial mesh size (12 m, 6 m, 3 m, 1.5 m, 0.75 m, 0.375 m etc.). As shown in Fig. 12, when the minimum mesh size reached to 0.375 m, the element number increased to 8,846,976, and this exceeded the computing ability of ordinary computer. Finally, considering the balance between computational efficiency and result accuracy, the minimum size of octree-based FDM mesh was set as 0.75 m.
3. A full tree with a uniform size of 0.75 m for the landslide analysis (see Fig. 20). The landslide analysis block model was then transformed into the FDM mesh in the typical profile. The critical slip surface searched by the dynamic programming method is a polyline between the FDM nodes. To get an accurate critical slip surface result, the mesh size should be as small as possible.

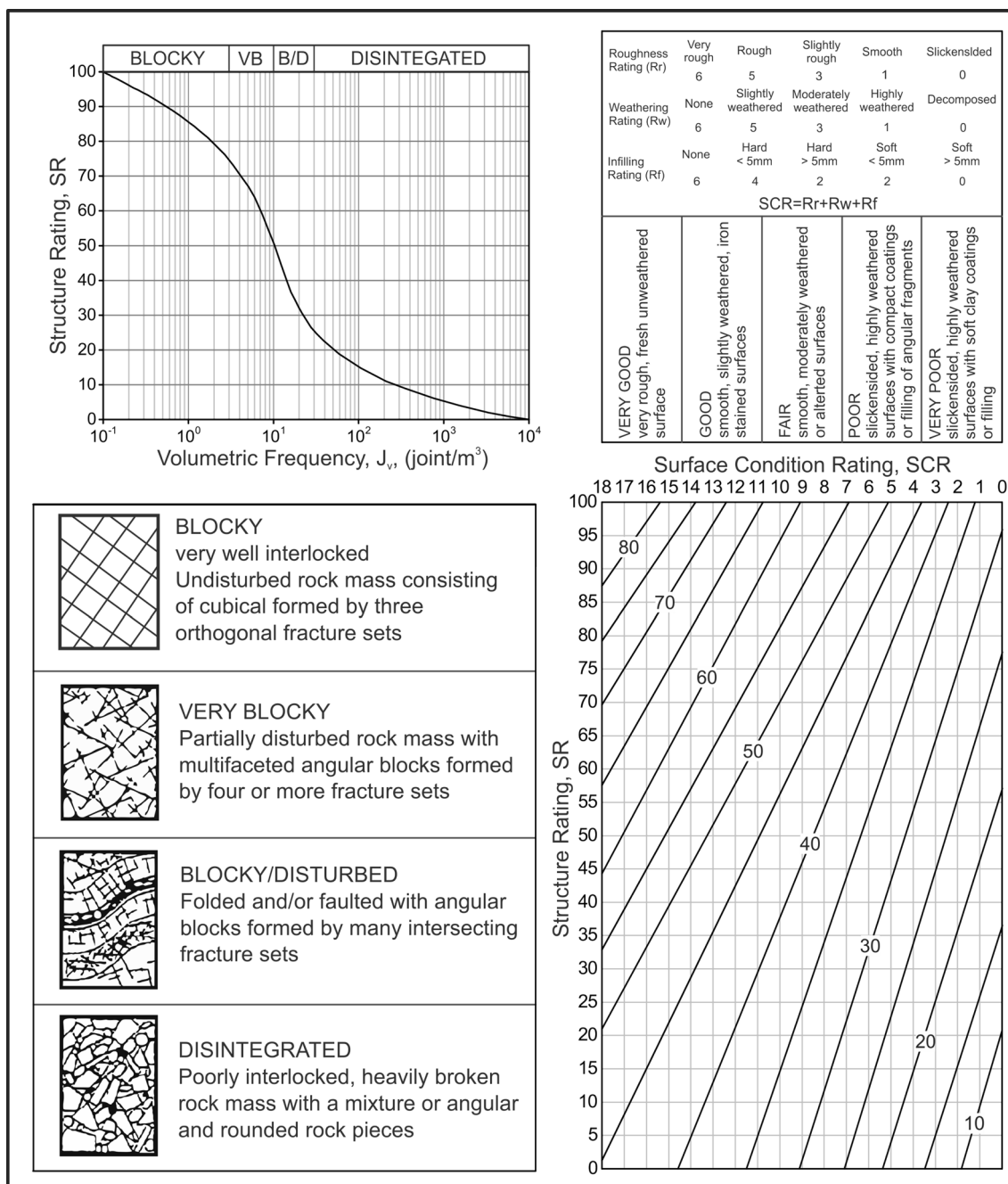


Fig. 8 Quantization of GSI system

ble within the calculation ability. Besides, the dynamic programming method performs better when the nodes of FDM mesh are evenly distributed. Finally, a full tree with a uniform size of 0.75 m was used. Since the typical profile was perpendicular to the ground and has an angle of 26.6° counterclockwise from the north direction. The size of FDM mesh for landslide analysis in the typical profile was 0.84 m in width and 0.75 m in height.

It is worth to notice that the block model with a smaller unit size can inherit the parameters from the superior block model. Those three block models share the same 3D geological model, but different block unit size, and that is the key and main principle for the octree-based method in this paper.

Table 2 Location accuracy tests of the MS monitoring system using blasting tests

Time	Location coordinate of blasting points (m)			Location coordinate in monitoring system (m)			Location error/m
	North	East	Altitude	North	East	Altitude	
2017/9/11	4,546,559.1	504,696.8	-222.4	4,546,566.1	504,688.2	-232.6	14.8
2017/9/11	4,546,475.4	504,697.9	-222.5	4,546,477.5	504,705.7	-220.6	8.3
2017/9/12	4,546,592.5	504,705.3	-222.2	4,546,587.1	504,687.8	-230	19.9
2017/10/11	4,546,621.5	504,861.7	-221.5	4,546,614.5	504,861.6	-214.4	10.0
2017/10/11	4,546,626.3	504,880.1	-222.2	4,546,631.1	504,889.8	-223.7	10.9
2017/10/12	4,546,640.6	504,846.9	-222.6	4,546,637.0	504,851.3	-226.3	6.8
2017/10/12	4,546,642.5	504,868.3	-222.3	4,546,651.6	504,877.7	-222.9	13.1

Fig. 9 MS monitoring system and spatial distribution of MS events. **(a)** MS monitoring system and monitoring result. MS spheres are sized by source energy and colored by moment magnitude. **(b)** Distribution of MS events in the typical profile. MS events are projected to the typical profile and sized by apparent volume

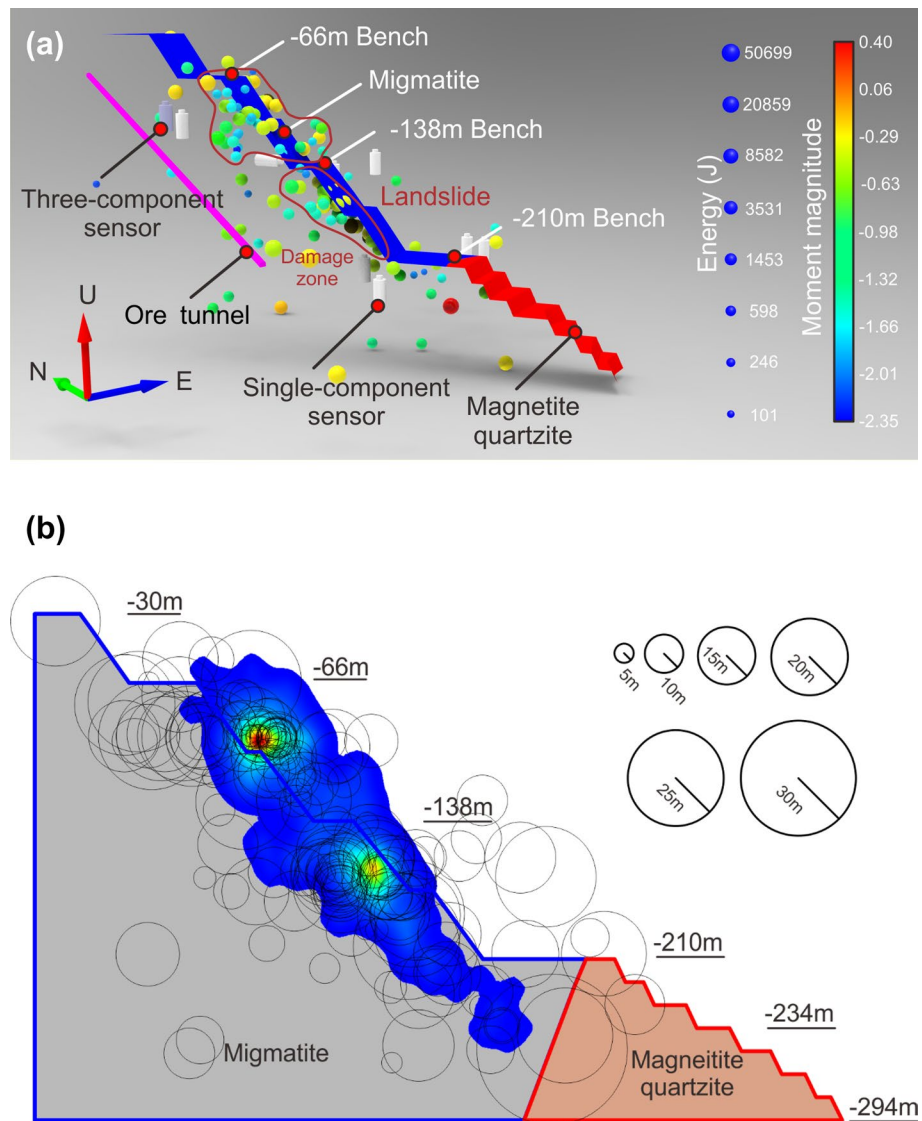
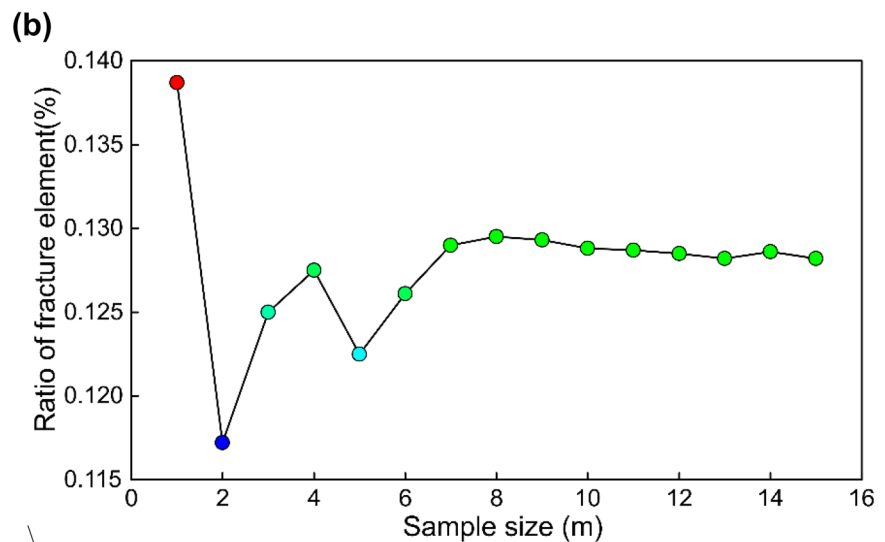
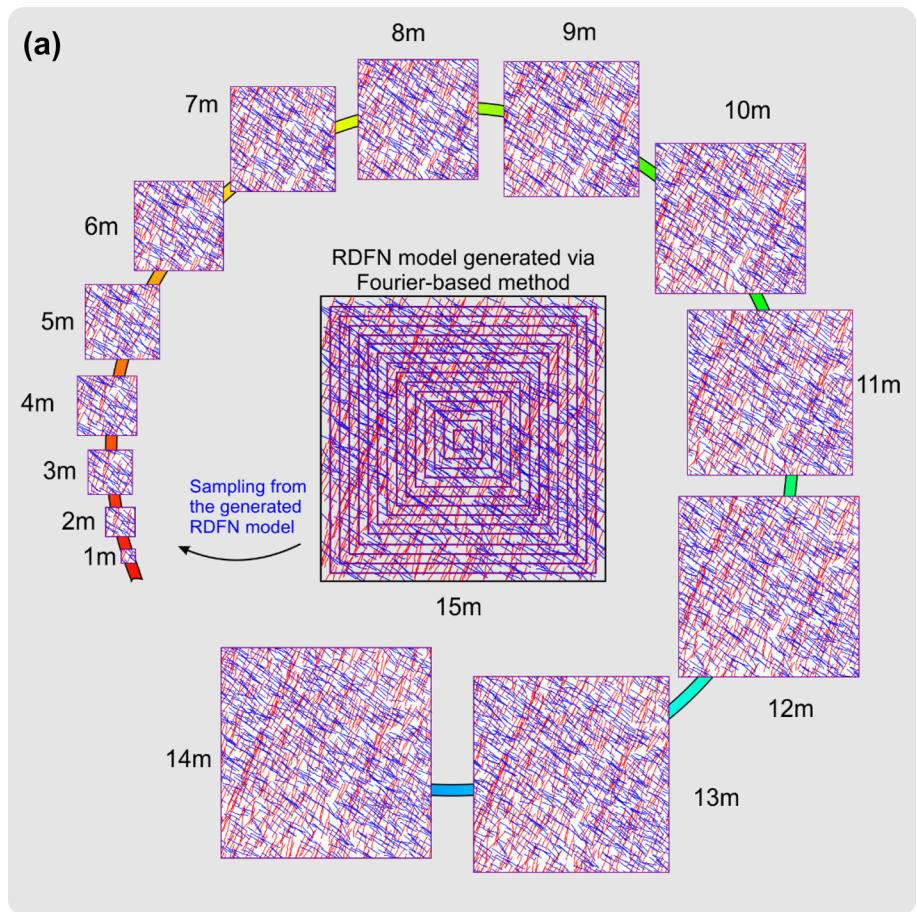


Fig. 10 REV determination of jointed rock mass. **(a)** Two-dimensional rough distract fracture network model. **(b)** Size effect of jointed rock mass



4 Spatial Variability and Time Decay Mechanical Parameters

4.1 Geostatistics-Based Assessment for the Spatial Variability

Geostatistical analysis techniques are used to evaluate the values of unknown points using sampling points, and geostatistical

methods are only valid for spatially dependent data. The basic method is to first identify and quantify the spatial structure of the variables of concern and then to interpolate or estimate the values of variables from neighboring values taking into account their spatial structure. Many researches have proven the volume frequency of discontinuity (Priest 1993; Caers 2005) and rock mass quality (Egaña and Ortiz 2013; Eivazy et al. 2017) follow certain geostatistical principle.

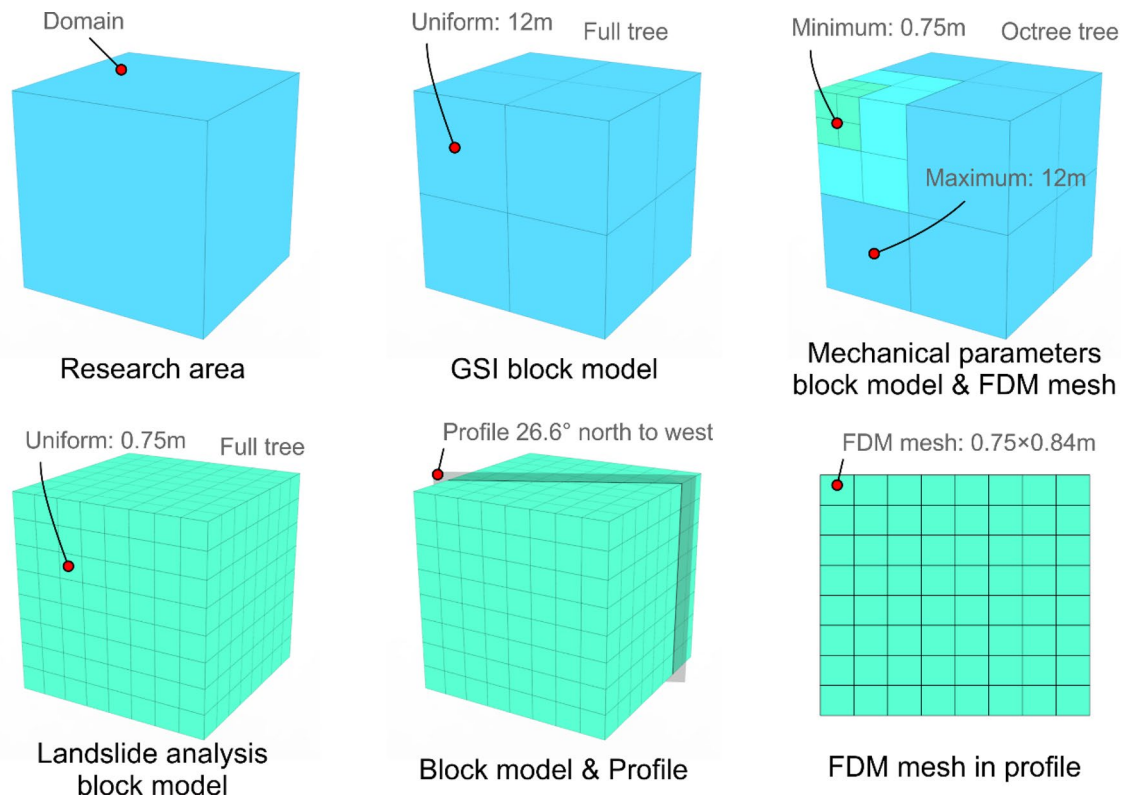


Fig. 11 Octree-based block model generation

There are many available methods including ordinary and universal kriging, inverse distance weighting (IDW), interpolating polynomials, splines, and power and Fourier series fitting are used to address the spatial interpolation. Compared with other methods, most notably kriging, the IDW method is not based on any mathematical or statistical assumptions; it is strictly intuitive. Regression, kriging interpolation method is based on specific statistical/mathematical assumptions (second-order stationarity conditions). In general, these assumptions may not be testable and certainly with a small number of data locations deciding whether the relevant assumptions are satisfied is more difficult. In the case of kriging, one of the critical steps is estimating the variogram and this is more difficult with a small number of sampling points. As for using statistical error tests to determine the best method it is likely that the statistical assumptions required by the tests will not be satisfied because the underlying assumptions are different for different interpolation methods, or in the case of IDW, there are no assumptions (Myers 1994; Adisoma and Hester 1996; Henley 2012). In this paper, only 94 GSI values are collected in the Dagushan open-pit mine, we cannot estimate an accurate semivariogram for the GSI, the IDW method is the appropriate choice to evaluate the GSI in each block unit. In fact, we can adopt different spatial interpolation method based on the abundance of sampling points. Kriging is employed to

handle GSI with abundant sampling points, and the IDW is applied when limited sampling points are available (Ferreira et al. 2017; Sajid et al. 2013).

The generic equation for IDW interpolation is as follows:

$$x_v = \frac{\sum_{i=1}^n \frac{x_i}{d_i^N}}{\sum_{i=1}^n \frac{1}{d_i^N}}, \tag{4}$$

where x_v is the point to be estimated, x_i is the i th sampling point, d_i is the distance between x_i and x_v . Besides, N is an exponent related the degree of variation. To minimize the

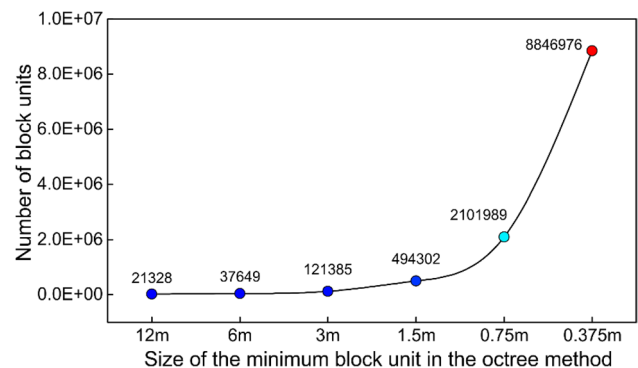


Fig. 12 Number of block units with different minimum block unit size using the octree method

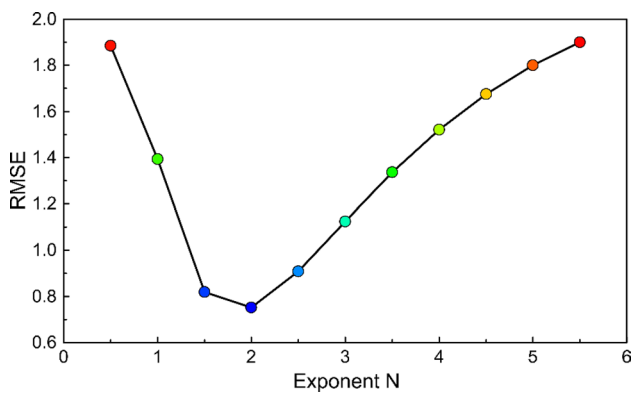


Fig. 13 RMSE with different exponent in the IDW method

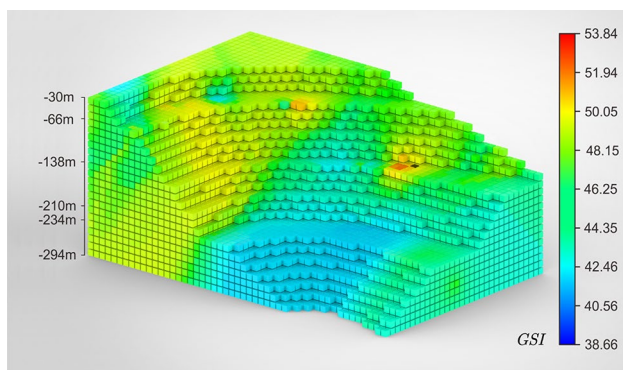


Fig. 14 Block model of GSI

estimation error, cross-validation is used to select an optimal exponent N from finite number of candidates (Tomczak 1998). The method is based on removing one sampling point at a time, performing the interpolation for the location of the removed point using the remaining samples, and calculating the residual between the measured value of the removed point and the estimate value for this point obtained from remaining samples. This scenario is repeated until every sample has been removed in turn. The overall performance of the interpolator is then evaluated as the root-mean of squared residuals (RMSE), and the exponent N with a lowest RMSE is taken as optimal:

$$RMSE = \sqrt{\frac{\sum_{i=1}^n (x_{i(int)} - x_i)^2}{n}}, \tag{5}$$

where RMSE is the root-mean-squared error, $x_{i(int)}$ is the interpolated value and x_i is the measured value.

As shown in Fig. 13, the optimal exponent in the Eq. (4) is 2 for the GSI interpolation process. The estimate result for GSI block model in the Dagushan open-pit mine is

shown in Fig. 14. Compared with the surrounding area, the GSI was lower (approximately 6–8) in the landslide zone. Inevitably, the lack of sampling points will bring estimation error of GSI, and it is hard to quantify this error in the IDW method. But we believe this error can be reduced with an appropriate interpolation method if enough sampling points are available. Compared with traditional rock mass quality classification method, our proposed method still can give a more detailed description for the spatial variability of GSI.

As we mentioned before, the GSI block model was next remeshed as a mechanical parameters block model. Using the octree method, the mesh can be divided small enough in the focused area without too many elements, which was beneficial for the accuracy and speed of numerical simulation. MATLAB codes were developed to implement the Hoek–Brown method in each mechanical parameter block unit. Four kind parameters, including intact rock parameters (density, UCS, Poisson’s ratio and material constant), GSI of rock mass, disturbance factor and buried depth of rock mass, are required in the Hoek–Brown method. The basic parameters of intact rock were obtained by laboratory experiment (see Table 1). The discontinuities were characteristics by GSI which were obtained by engineering geological survey (see Sect. 2.3) and geostatistics-based estimation (see Sect. 4.1). Since the blast was well controlled in the Dagushan open-pit mine, the blast damage factor was ignored throughout this study and a constant value of 0.0 used. Besides, gradient growth height of the slope in each element was taken into account. As shown in Fig. 15, the mechanical parameters obtained by the Hoek–Brown method were mainly controlled by the lithology and buried depth. Besides, lower rock mass quality led poor mechanical parameters in the landslide zone. The mechanical parameters varied widely even within the same lithology, which indicated the mechanical parameters have an obvious spatial variability characteristic in the Dagushan open-pit mine.

4.2 MS-Driven Damage Model for the Time Decay

To analyse the time decay characteristic of rock mass mechanical parameters under the influence of mining activities, a damage model driven by MS data was proposed to describe the rock mass failure process based on the energy dissipation theory. The degree of damage and dimension of the damage zone can be quantized by the MS-driven damage model.

The rock mass is assumed as a closed isotropic system. According to the first law of thermodynamics (Xie et al. 2005)

$$U = U_E + U_D, \tag{6}$$

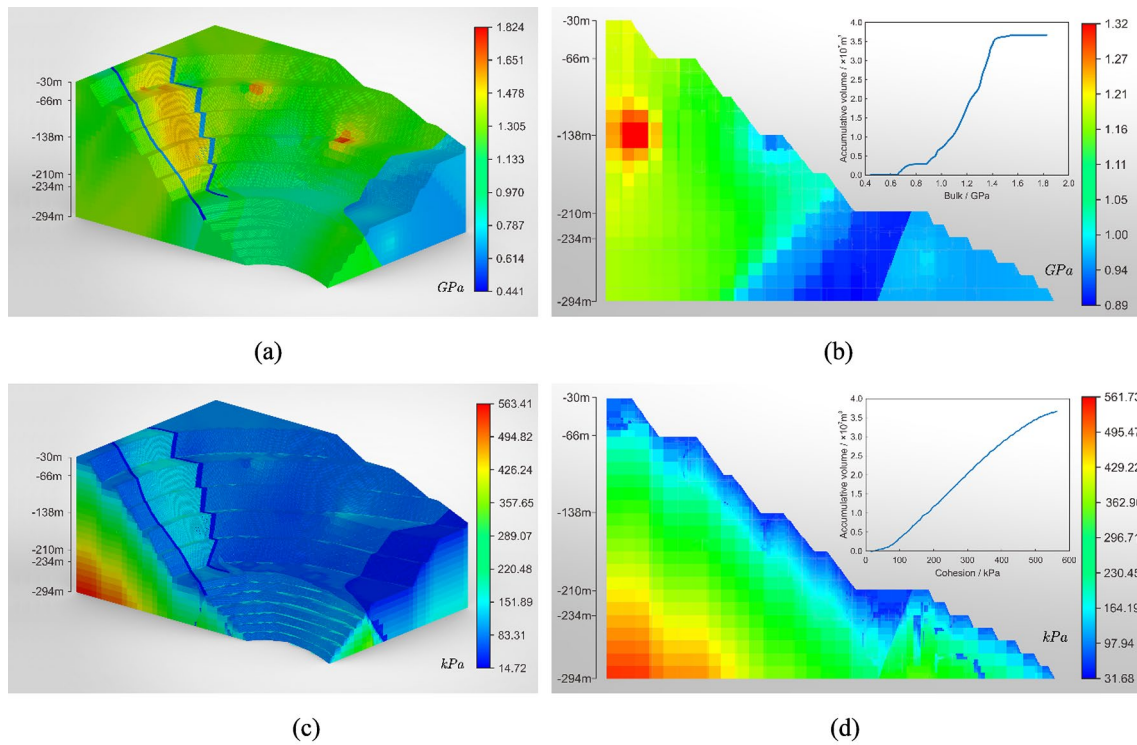


Fig. 15 Block model of spatial variability mechanical parameters. **(a)** Bulk modulus. **(b)** Bulk modulus in the typical profile. **(c)** Cohesion. **(d)** Cohesion in the typical profile

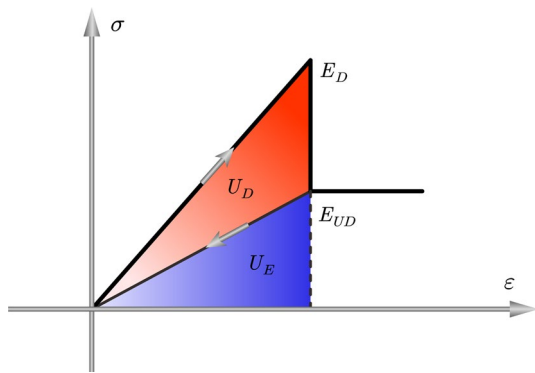


Fig. 16 Quantitative relationship between energy release and energy dissipation in an elastic-brittle rock mass unit

where U is the total energy exercised by external forces on rock mass unit, U_E is the releasable strain energy and U_D is the dissipation energy. In this paper, we assumed that the deformation behaviour in each rock mass unit follows the elastic-brittle process. The relationship between the releasable strain energy U_E and the dissipation energy U_D in a rock mass unit is shown in Fig. 16. E_{UD} is the initial elastic modulus of the rock mass unit, and E_D is the elastic modulus of the damaged rock mass unit.

The total energy of rock mass unit in the principal stress space can be expressed as follows:

$$U = \frac{1}{2E_{UD}} [\sigma_1^2 + \sigma_2^2 + \sigma_3^2 - 2\nu(\sigma_1\sigma_2 + \sigma_2\sigma_3 + \sigma_1\sigma_3)], \quad (7)$$

where $\sigma_1, \sigma_2, \sigma_3$ is, respectively, the maximum, medium and minimum principal stress and ν is Poisson's ratio.

During the failure process, the dissipation energy U_D stored in a rock mass unit was released and transformed into the kinetic energy, MS energy et al. The MS energy, U_M , can be obtained by the MS monitoring equipment, and then it was evenly assigned into each rock mass unit located in the damage zone. The MS energy was considered to occupy a fixed part of dissipation energy (Sagasta et al. 2016):

$$U_M = \eta U_D, \quad (8)$$

where η is the seismic efficiency and can be obtained by blast tests.

The degree of damage can be represented by the damage variable D , and the damage variable D of a single rock mass unit within seismic source dimension can be defined as follows:

$$D = \frac{U_D}{U} = \frac{U_M}{\eta U}. \quad (9)$$

The elastic modulus of damage rock mass unit can be expressed as follows:

$$E_D = E_{UD}(1 - D). \tag{10}$$

By bringing Eqs. (7) and (9) into Eq. (10), the elastic modulus of damaged rock mass unit can be obtained as follows:

$$E_D = \left\{ 1 - \frac{2E_{UD}U_M}{\eta[\sigma_1^2 + \sigma_2^2 + \sigma_3^2 - 2\nu(\sigma_1\sigma_2 + \sigma_2\sigma_3 + \sigma_1\sigma_3)]} \right\} E_{UD}, \tag{11}$$

where σ_1 , σ_2 and σ_3 can be obtained by numerical simulation, and U_M can be monitored by the MS system.

Additionally, we assumed that the cohesion and friction angle share the same damage variable with elastic modulus (Martin and Chandler 1994):

$$\begin{aligned} c_D &= c_{UD}(1 - D) \\ \tan \varphi_D &= \tan \varphi_{UD}(1 - D) \end{aligned} \tag{120}$$

Apparent volume is the volume of seismic source with inelastic deformation, which can be calculated as follows (Cai et al. 1998):

$$V_A = \frac{M^2}{2GE_{MS}}, \tag{13}$$

where V_A is the apparent volume, M is the seismic moment and G is the rock stiffness; E_{MS} is the source seismic energy, and the relationship between E_{MS} and U_M is as follows:

$$E_{MS} = \sum_{i=1}^N U_M^i, \tag{14}$$

where N is the number of rock mass unit located in the range of MS apparent volume.

Assuming the apparent volume of MS events is an isotropic sphere, the dimension of damage zone is defined as follows:

$$R = \sqrt[3]{\frac{3M^2}{8\pi GE}}. \tag{15}$$

Therefore, the source dimension R is used to quantify the damage dimension of rock mass corresponding to the MS events. The elastic modulus, cohesion and friction of the rock mass units within the distance R of the MS event location were weakened by the damage model.

As shown in Table 3, seven blast tests were employed to determine the seismic efficiency. Assuming the damage variable $D = 1$ in the apparent volume of a blast event, which means rock mass unit is completely damaged:

$$\sum_{i=1}^N U^i = \sum_{i=1}^N U_D^i = \sum_{i=1}^N \frac{U_M^i}{\eta} = \frac{E_{MS}}{\eta}. \tag{16}$$

The average seismic efficiency can be calculated as 1.8508%. Therefore, in the research area of the Dagushan open-pit mine, only 1.8508% of the energy released during rock mass failure was spread in the way of elastic wave and received by MS sensors.

An initial stress field was obtained with the Mohr–Coulomb model in FLAC. The boundary conditions for the FDM model are listed as follows: the vertical displacements are fixed in the bottom boundary, and the displacements at the normal direction are fixed for the vertical boundaries. Besides, other slope surfaces are set as free. Then, the damage model driven by MS data was implemented in the FLAC software by using the FISH language. According to the location, energy and apparent volume of MS events in the area, the MS events were mapped to the numerical simulation. The code can automatically search and weaken mechanical parameters of rock units within the damage scope of MS events. Figure 17a gives a damage field of the research area, and the damage field in the typical profile is shown in Fig. 17b. Additionally, time decay mechanical parameters based on MS events are shown in Fig. 18. Due to the MS events concentrated in the landslide zone, the rock mass mechanical parameters were further weakened which led to final rock landslide.

Table 3 Acquisition of seismic efficiency based on blast tests

Time	Maximum principle stress (Pa)	Intermediate principal stress (Pa)	Minimum principle stress (Pa)	Elastic modulus (Pa)	Poisson's ratio	Apparent volume (m ³)	Dissipation energy (J)	MS energy (J)	Seismic efficiency (%)
2017/9/11	5.17E+05	4.69E+05	3.02E+05	1.82E+09	0.21	5.41E+04	5.23E+06	8.51E+04	1.6264
2017/9/11	4.05E+05	3.38E+05	2.50E+05	1.50E+09	0.23	1.44E+04	9.24E+05	2.26E+04	2.4497
2017/9/12	3.92E+05	2.91E+05	2.46E+05	1.49E+09	0.23	2.15E+04	1.22E+06	3.39E+04	2.7765
2017/10/11	5.05E+05	1.92E+05	-1.05E+04	1.46E+09	0.23	4.30E+04	3.70E+06	6.76E+04	1.8295
2017/10/11	5.54E+05	4.43E+05	-9.57E+04	1.47E+09	0.23	6.84E+04	1.03E+07	1.08E+05	1.0447
2017/10/12	4.19E+05	2.29E+05	-7.18E+04	1.45E+09	0.23	3.86E+04	2.80E+06	6.07E+04	2.1698
2017/10/12	5.34E+05	4.64E+05	-7.57E+04	1.44E+09	0.23	7.64E+04	1.14E+07	1.20E+05	1.0590

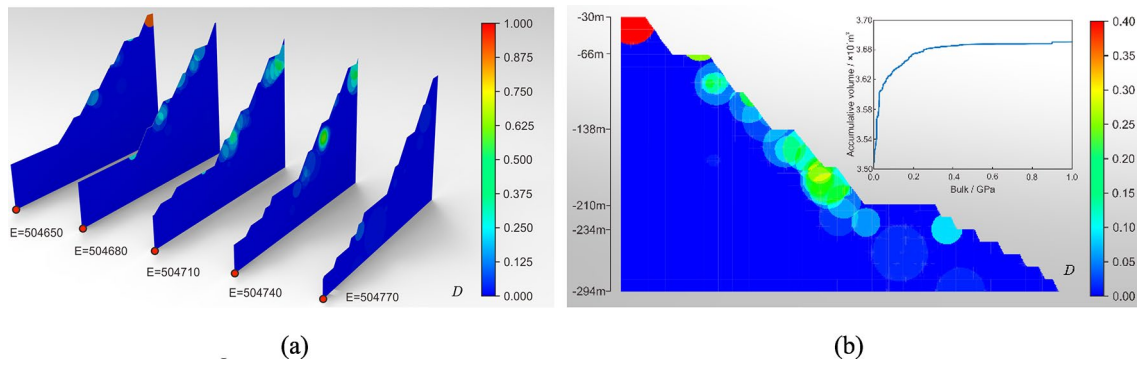


Fig. 17 Damage field driven by MS data. (a) Damage variable. (b) Damage variable in the typical profile

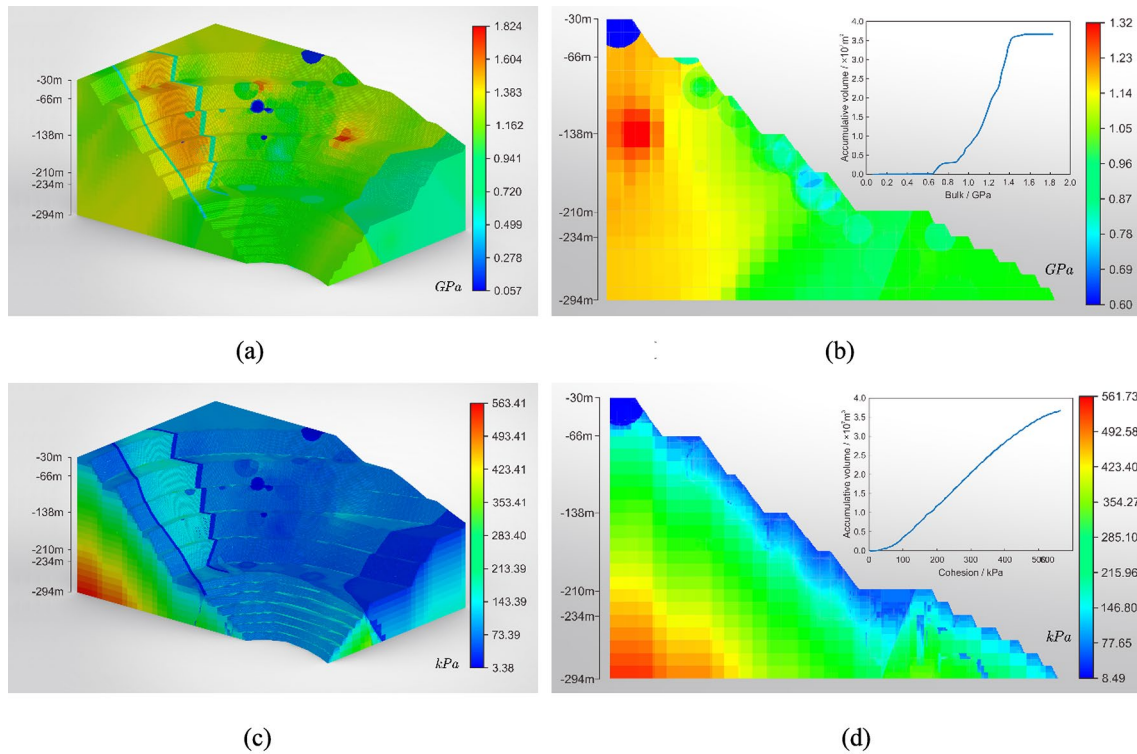


Fig. 18 Block model of time decay mechanical parameters. (a) Bulk modulus. (b) Bulk modulus in the typical profile. (c) Cohesion. (d) Cohesion in the typical profile

5 Landslide Analysis Using Dynamic Programming Method

5.1 Theory of the Dynamic Programming Method

As shown in Fig. 19a, for an arbitrary critical slip surface in two-dimensional space, the safety factor f_s can be obtained by Eq. (17):

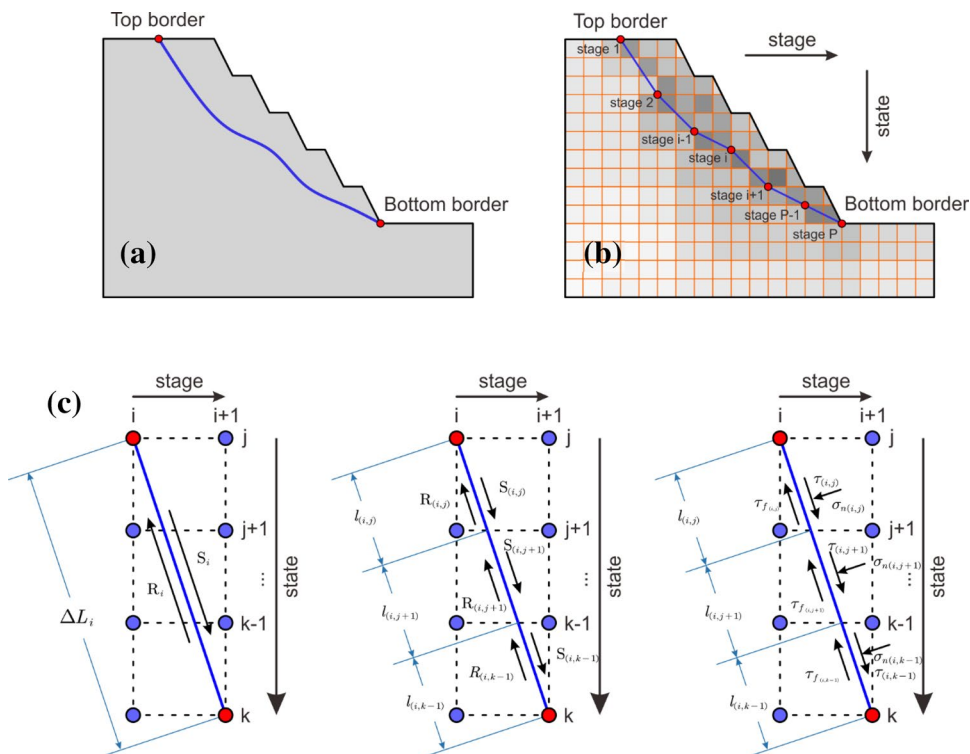
$$f_s = \frac{\int_{\text{Bottom}}^{\text{Top}} \tau_f dL}{\int_{\text{Bottom}}^{\text{Top}} \tau dL}, \tag{17}$$

where τ is the mobilized shear stress along the critical slip surface, and τ_f is the shear strength of the rock mass. As shown in Fig. 19b, we divided the critical slip surface into several stages, and the safety factor can be defined as follows:

$$f_s = \frac{\sum_{i=1}^P \tau_{fi} \Delta L_i}{\sum_{i=1}^P \tau_i \Delta L_i}, \tag{18}$$

where P is the number of discrete stages, and ΔL_i is the length of the critical slip surface in the i th stage.

Fig. 19 Search for the critical slip surface based on the dynamic programming method. **a** An arbitrary surface; **b** an arbitrary surface in the discretized form; **c** actuating and resisting forces acting on the *i*th stage



As shown in Fig. 19c, to determine a critical slip surface with a minimum safety factor, an auxiliary function is defined as follows:

$$G_m = \min \sum_{i=1}^P (R_i - f_s S_i), \tag{19}$$

where S_i is the actuating force acting on the *i*th stage of the critical slip surface, and R_i is the resisting forces acting on the *i*th stage of the critical slip surface. We assume that rock mass obeys the perfectly plastic Mohr–Coulomb failure criterion:

$$\tau_{fi} = c_i + \sigma_{ni} \tan \varphi_i, \tag{20}$$

where σ_{ni} is the normal stress, c_i is the cohesion and φ_i is the friction of rock mass in the *i*th stage. The normal and shear stresses acting on the *i*th stage can be computed from a stress analysis in two-dimensional space (it was noticed that the positive for compressive stress and negative for tensile stress in rock mechanics) as follows:

$$\begin{aligned} \sigma_n &= \sigma_x \sin^2 \theta + \sigma_y \cos^2 \theta - \tau_{xy} \sin 2\theta \\ \tau_f &= \tau_{xy} (\sin^2 \theta - \cos^2 \theta) - \frac{(\sigma_y - \sigma_x)}{2} \sin 2\theta \end{aligned} \tag{21}$$

where θ is the inclined angle of the *i*th stage with the horizontal direction, and σ_x , σ_y and τ_{xy} can be determined with any stress analysis software. Then, the actuating and resisting forces acting on the *i*th stage of a critical slip surface can be calculated with Eq. (22):

$$\begin{aligned} S_i &= \sum_{j=1}^{Q_i} S_{(i,j)} = \sum_{j=1}^{Q_i} \tau_{(i,j)} l_{(i,j)} \\ R_i &= \sum_{j=1}^{Q_i} R_{(i,j)} = \sum_{j=1}^{Q_i} \tau_{f(i,j)} l_{(i,j)} \quad , \\ &= \sum_{j=1}^{Q_i} \left[c_{(i,j)} + \sigma_n^{(i,j)} \tan \phi_{(i,j)} \right] l_{(i,j)} \end{aligned} \tag{22}$$

where (i, j) is element across the critical slip surface in the *i*th segment, and Q_i is the number of (i, j) . Considering the kinematically admissible, the resisting force and the actuating force along the slip surface must be in contrary directions.

An optimal function, $H_i(j)$, obtained at state point $\{j\}$ located in stage $[i]$ is introduced. The optimal function is equal to the minimum value of auxiliary function G_m between the initial stage and stage point $\{j\}$ located in stage $[i]$. According to the principle of optimality (Richard 1957), the optimal function, $H_{i+1}(k)$, obtained at state point $\{k\}$ located in stage $[i + 1]$ is defined as follows:

$$H_{i+1}(k) = H_i(j) + G_i(\overline{j, k}), \tag{23}$$

where $G_i(\overline{j, k})$ is the auxiliary function calculated from state point $\{j\}$ of stage $[i]$ to state point $\{k\}$ of stage $[i + 1]$. At the initial stage, the value of the optimal function is equal to zero, and at the final stage, the optimal function is equal to the minimum value of the auxiliary function.

$$H_1(j) = 0 \quad j = 1, 2, \dots, Q_1$$

$$H_p(k) = G_m = \min \sum_{i=1}^P (R_i - f_s S_i) \quad i = 1, 2, \dots, Q_p \quad (24)$$

The optimal point in the final stage is defined as the state point at which the calculated optimal function is a minimum. It is worth noticing that only the state points under the slope surface have the opportunity to be chosen. From the optimal state point $\{k\}$ found in the final stage, the optimal state point $\{j\}$ located in the previous stage is also determined. The optimal path defined by connecting optimal state points located in every stage is eventually found by tracing back from the final stage to the initial stage. This optimal path defines the critical slip surface. The value of the overall factor of safety, f_s , in Eq. (19) should be assumed with an initial value (usually the initial value is set as 1). The trial value of f_s is updated using the value of f_s that is evaluated after each trial of the search. The optimization process will stop when a predefined convergence is reached.

5.2 Landslide Analysis in the Typical Profile

The present dynamic programming method is only suitable for two-dimensional slope stability analyses. As shown in Fig. 2, a typical profile with the rock landslide was selected. The stresses were computed using FLAC with Mohr–Coulomb model, and the stress at the centre point of each element was interpolated using the surrounding nodes. The stress-interpolation process was done prior to the performance of the dynamic programming search. The grid with corresponding stress was imported to the open source code DYNPROG developed by Pham and Fredlund (2003). Since the optimization search for the dynamic programming method was performed on a grid of stage-state points (referred to the search grid). In this paper, the FDM mesh was also set as the search grid. The top and bottom border of landslide obtained by engineering investigation was set as the entry and exit point for the critical slip surface. DYNPROG can search a critical slip surface and factor of safety automatically.

Following the flowchart shown in Fig. 1c, three different mechanical parameters conditions in the typical profile were studied to illustrate the rationality of the mechanical parameters block model: (1) Homogeneous model: the rock mass unit was sorted into two discrete homogeneous domains based on the lithology, and the mechanical parameters were set as the average value in each domain. (2) Spatial variability model: heterogeneous mechanical parameters considering the spatial variability but without considering the time decay. (3) Time decay model: heterogeneous mechanical parameters considering both the spatial variability and the

time decay. The slope stability analysis results are shown in Fig. 20.

Incorporation of spatial variability and time decay into mechanical parameters resulted in a fundamental change in the slope stability. For the homogeneous model, shear stresses were typically concentrated at the toe of each bench slope with a smooth stress contour. However, strong spatial heterogeneous characteristic of the rock mass led to a complicated stress state, especially in the landslide zone. By considering the time decay mechanical parameters, the stress of MS-driven damage area (from bench – 66 m to bench – 210 m) was lower compared with the undamaged model (see max shear stress field in Fig. 20).

All the critical slip surface in three mechanical parameters conditions featured the characteristics of decline rapidly near the top border, slide straightly in the middle and remain rough near the bottom border, which suggested that failure was generally geometry controlled in rock slope. For the spatial heterogeneous models, rough critical slip surface searched by the dynamic programming method indicated that failure was preferential to the weakest areas of the rock mass, and the characteristic of time decay exacerbated this tendency. In comparison, the rock mass affected by critical slip surface both considering spatial variability and time decay has an average reduction of 15–30% in strength and elastic modulus compared with undamaged area (see Figs. 17b, 20). This preference led the main difference among those three critical slip surfaces, i.e. the depth and area of slide body. Compared with the heterogeneous model (12.5 m), heterogeneity led to a deeper slide body especially in the top border of landslide (13.5 m for spatial variability model, 15.4 m for time decay model). Besides, with the similar length of critical slip surface, the area of slide body in the typical profile has an obvious difference (1034.5 m² for heterogeneous model, 981.7 m² for spatial variability model and 1131.0 m² for time decay model). Engineering investigation showed there is a large vertical settlement of the slide body in the top border of landslide. We believe the critical slip surface considering both spatial variability and time decay mechanical parameters have a good corresponding with the in-situ engineering.

A critical component of any stability analysis is estimation of the mechanical parameters of the rock mass and the critical slip surface that control sliding. Landslide analysis with homogeneous mechanical parameters ignored inevitably overestimates the safety factor. Compared with homogeneous model, the application of geostatistics and MS-driven damage model provided more detailed mechanical parameters, and this shift resulted in a reduction of the factor of safety from 1.444 in the homogeneous model, to 1.143 within the geostatistics-based spatial variability model and 0.974 within the MS-driven time decay model.

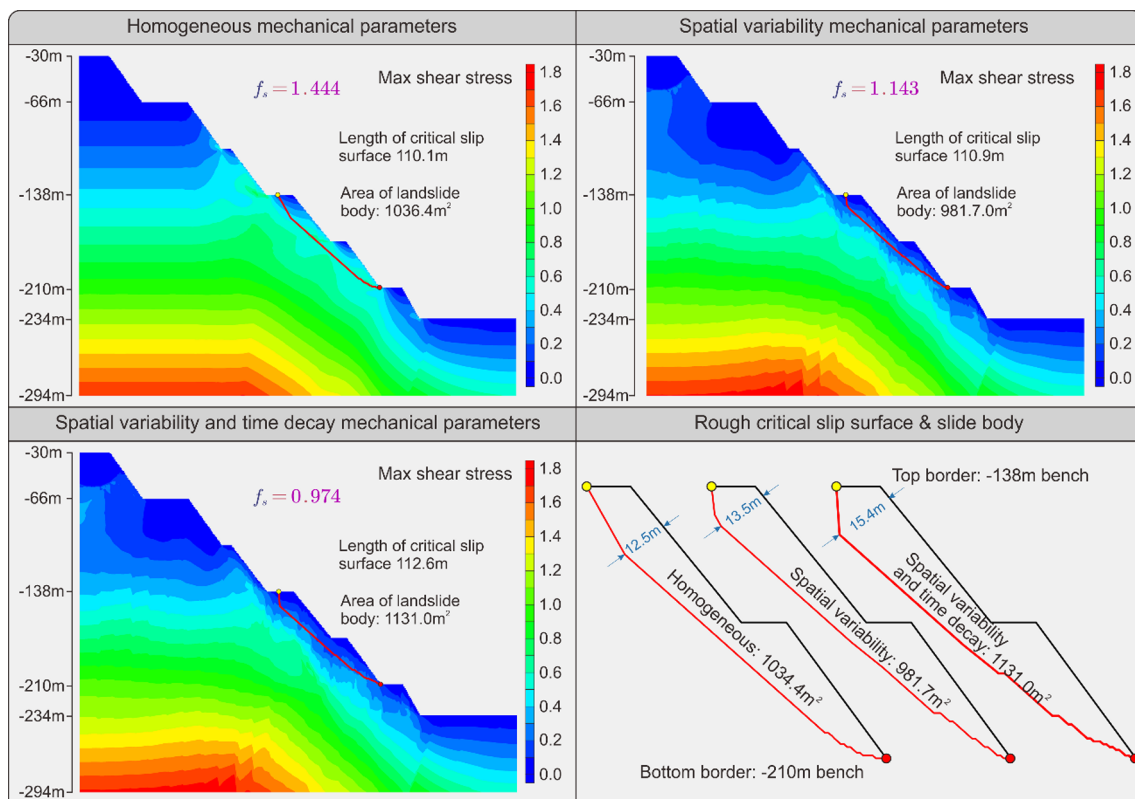


Fig. 20 Slope stability analysis result in the typical profile

Theoretically, the factor of safety should be smaller than 1 under the landslide. The shift of safety factor under different mechanical parameter conditions can verify the rationality of the proposed rock mass property modification method.

5.3 Discussion

1. Due to the optimization search for the dynamic programming method was performed on the discrete nodes of FDM mesh, the grid size might affect the results of slope stability analysis result. Theoretically, to get a more accurate critical slip surface and factor of safety, the mesh size should be as small as possible within the calculation ability. On Pham and Fredlund's (2003) previous work, four densities of the search grid were examined for a slope at $70\text{ m} \times 40\text{ m}$, including the coarse ($5\text{ m} \times 1\text{ m}$) grid, the medium ($2\text{ m} \times 0.5\text{ m}$) grid, the fine ($2\text{ m} \times 0.25\text{ m}$) grid and the dense ($1\text{ m} \times 0.25\text{ m}$) grid. The result indicated that the density of the search grid does not seriously affect the factor of safety. Besides, Baker (1980) suggested that the ratio of the distance between two state points over the distance between two successive stage points should be about one to four. In this paper, the FDM mesh was set as $0.84 \times 0.75\text{ m}$, have
2. a ratio of 1.12, which corresponds to the medium or fine grid in Pham and Fredlund's (2003) work. Besides, the slope stability analysis result has a good corresponding to the engineering investigation. We believe that the octree-based FDM mesh can meet the need of dynamic programming method in this paper.

2. For the Dagushan open-pit mine, the mining depth has reached 450 m in 2019, mine operations are progressing towards ever deeper targets in response to the depletion of near-surface deposits. A single degree increase of the slope angle will save millions of dollars of stripping costs; unfortunately, the economic benefits gained can be negated by major slope failure. A critical component of any stability analysis is estimation of the mechanical parameters of the rock mass. The proposed geostatistics-based method and MS-driven damage model are used to character the spatial variability and time decay of rock mass mechanical parameter. Although the proposed approach is more data intensive and difficult to apply, the inability to account for spatial heterogeneous in the geological data and damage process of the rock mass may lead to systematic errors, invalid results and poor designs.

6 Conclusions

In this paper, a geostatistics-based method and a MS-driven damage model were proposed to characterize the spatial variability and time decay of rock mass mechanical parameters. Additionally, by combined heterogeneous mechanical parameters and stress state, the dynamic programming method was used to search the rough critical slip surface and the factor of safety. A detailed engineering geological survey and a long-period MS monitoring system provided a suitable application scene in the Dagushan open-pit mine.

1. Focusing on the spatial distribution of rock mass quality GSI, the geostatistics-based method and Hoek–Brown method allow us to obtain more detailed spatial variability mechanical parameters from limited sampling data. Moreover, the MS-driven damage model based on energy dissipation theory can quantify the damage location, extent and dimension, thus providing the time decay mechanical parameters of rock masses.
2. Compared with the homogeneous model, incorporation of spatial variability and time decay into mechanical parameters resulted in a more reasonable slope stability analysis result, both in the critical slip surface and factor of safety. Rough critical slip surface for the heterogeneous model was preferred to pass through the area with weak mechanical parameters. Besides, engineering investigation indicated that ignoring of heterogeneity inevitably overestimates the safety factor.
3. Instead of relying on ambiguous geological and engineering judgment, the block model generated by octree-based method can give a detailed characterization to the heterogeneity of rock mass. Furthermore, the block model can transform into FDM mesh without many processes, which simplified the pre-processing for the numerical simulation.

Acknowledgements This work was supported by the National Key Research and Development Program of China (2016YFC0801602 and 2017YFC1503101), the National Science Foundation of China (U1710253, 51574059 and 51574060) and the China Scholarship Council (201806080101). We would like to thank Professor Peijun Guo from McMaster University for his guidance and support, and Andy Yan, Li Xu and Dylan Liu from McMaster University for their help in English writing. We also would like to thank anonymous reviewers and the editor for constructive comments that helped improve this manuscript.

References

Adisoma GS, Hester MG (1996) Grade estimation and its precision in mineral resources: the Jackknife approach. *Min Eng* 48(2):84–88

- Baker R (1980) Determination of the critical slip surface in slope stability computations. *Int J Numer Anal Meth Geomech* 4:333–359
- Bazant ZP, Belytschko TB, Chang TP (1984) Continuum theory for strain-softening. *J Eng Mech* 110:1666–1692
- Caers J (2005) *Petroleum geostatistics*. Soc. of Petroleum Eng, Richardson
- Cai M, Kaiser PK, Martin CD (1998) A tensile model for the interpretation of microseismic events near underground opening. *Pure Appl Geophys* 153:67–92
- Cai M, Kaiser PK, Martin CD (2001) Quantification of rock mass damage in underground excavations from microseismic event monitoring. *Int J Rock Mech Min Sci* 38:1135–1145
- Cai M, Morioka H, Kaiser PK, Tasaka Y, Kurose H, Minami M, Maejima T (2007) Back-analysis of rock mass strength parameters using AE monitoring data. *Int J Rock Mech Min Sci* 44:538–549
- Cristescu ND, Hunsche U (1998) *The time effects in rock mechanics*. Wiley, New York
- Egaña M, Ortiz JM (2013) Assessment of RMR and its uncertainty by using geostatistical simulation in a mining project. *J GeoEng* 8:83–90
- Eivazy H, Esmaili K, Jean R (2017) Modelling geomechanical heterogeneity of rock masses using direct and indirect geostatistical conditional simulation methods. *Rock Mech Rock Eng* 50:3175–3195
- Fakhimi A, Fairhurst C (1994) A model for the time-dependent behavior of rock. *Int J Rock Mech Min Sci Geomech Abstr* 31(2):117–126
- Feng XT, Zhang Z, Sheng Q (2000) Estimating mechanical rock mass parameters relating to the Three Gorges Project permanent shiplock using an intelligent displacement back analysis method. *Int J Rock Mech Min Sci* 37:1039–1054
- Fenton GA, Griffiths VD (2008) *Risk assessment in geotechnical engineering*. Wiley, New York
- Ferreira IO, Rodrigues DD, Santos GRD, Rosa LMF (2017) In bathymetric surfaces: IDW or Kriging? *Boletim de Ciências Geodésicas* 23:493–508
- Griffiths DV, Huang J, Fenton GA (2009) Influence of spatial variability on slope reliability using 2-D random fields. *J Geotech Geoenviron Eng* 135:1367–1378
- Henley S (2012) *Nonparametric geostatistics*. Applied Science Publishers Ltd, London
- Hoek E (2007) *Practical rock engineering*. <https://www.rocksolid.com>
- Hoek E, Carranza-Torres C (2002) Hoek–Brown failure criterion—2002 edition. In: *Proceedings of the fifth North American rock mechanics symposium*, vol 1, pp 18–22
- Jiang SH, Li DQ, Zhang LM, Zhou CB (2014) Time-dependent system reliability of anchored rock slopes considering rock bolt corrosion effect. *Eng Geol* 175:1–8
- Kanit T, Forest S, Galliet I, Mounoury V, Jeulin D (2003) Determination of the size of the representative volume element for random composites: statistical and numerical approach. *Int J Solids Struct* 40:3647–3679
- Lebert F, Bernardie S, Mainsant G (2011) Hydroacoustic monitoring of a salt cavity: an analysis of precursory events of the collapse. *Nat Hazards Earth Syst Sci* 11:2663–2675
- Lee YK, Pietruszczak S (2008) A new numerical procedure for elastoplastic analysis of a circular opening excavated in a strain-softening rock mass. *Tunn Undergr Space Technol* 23:588–599
- Li DQ, Jiang SH, Cao ZJ, Zhou W, Zhou CB, Zhang LM (2015) A multiple response-surface method for slope reliability analysis considering spatial variability of soil properties. *Eng Geol* 187:60–72
- Ma T, Tang C, Tang L, Zhang W, Wang L (2015) Rockburst characteristics and microseismic monitoring of deep-buried tunnels for Jinping II Hydropower Station. *Tunn Undergr Space Technol* 49:345–368
- Malan D (1999) Time-dependent behaviour of deep level tabular excavations in hard rock. *Rock Mech Rock Eng* 32:123–155

- Maranini E, Yamaguchi T (2001) A non-associated viscoplastic model for the behaviour of granite in triaxial compression. *Mech Mater* 33:283–293
- Martin C, Chandler N (1994) The progressive fracture of Lac du Bonnet granite. *Int J Rock Mech Min Sci Geomech Abstr* 31:643–659
- Mayer JM, Stead D (2017) A comparison of traditional, step-path, and geostatistical techniques in the stability analysis of a large open pit. *Rock Mech Rock Eng* 50:927–949
- Myers DE (1994) Spatial interpolation: an overview. *Geoderma* 62:17–28
- Pham HT, Fredlund DG (2003) The application of dynamic programming to slope stability analysis. *Can Geotech J* 40:830–847
- Priest SD (1993) *Discontinuity analysis for rock engineering*. Chapman & Hall, London
- Read J, Stacey P (2018) *Guidelines for open pit slope design*. CSIRO Publishing, Collingwood
- Reindu JM (1978) *An introduction to geostatistical methods of mineral evaluation*. South African Institute of Mining and Metallurgy
- Richard B (1957) *Dynamic programming*. Princeton University Press, 89:92
- Sagasta F, Benavent-Climent A, Roldán A, Gallego A (2016) Correlation of plastic strain energy and acoustic emission energy in reinforced concrete structures. *Appl Sci* 6:84
- Sajid A, Rudra R, Parkin G (2013) Systematic evaluation of kriging and inverse distance weighting methods for spatial analysis of soil bulk density. *Can Biosyst Eng* 55:1–13
- Sharifzadeh M, Tarifard A, Moridi MA (2013) Time-dependent behavior of tunnel lining in weak rock mass based on displacement back analysis method. *Tunn Undergr Space Technol* 38:348–356
- Sonmez H, Ulusay R (1999) Modifications to the geological strength index (GSI) and their applicability to stability of slopes. *Int J Rock Mech Min Sci* 36:743–760
- Stavropoulou M, Exadaktylos G, Saratsis G (2007) A combined three-dimensional geological-geostatistical-numerical model of underground excavations in rock. *Rock Mech Rock Eng* 40:213–243
- Tang C (1997) Numerical simulation of progressive rock failure and associated seismicity. *Int J Rock Mech Min Sci* 34:249–261
- Tomczak M (1998) Spatial interpolation and its uncertainty using automated anisotropic inverse distance weighting (IDW)-cross-validation/jackknife approach. *J Geogr Inf Decis Anal* 2:18–30
- Wang S, Zheng H, Li C, Ge X (2011) A finite element implementation of strain-softening rock mass. *Int J Rock Mech Min Sci* 48:67–76
- Xie H, Ju Y, Li L (2005) Criteria for strength and structural failure of rocks based on energy dissipation and energy release principles. *Chin J Rock Mech Eng* 24:3003–3010 (in Chinese)
- Xu N, Dai F, Liang Z, Zhou Z, Sha C, Tang C (2014) The dynamic evaluation of rock slope stability considering the effects of microseismic damage. *Rock Mech Rock Eng* 47:621–642
- Yerry MA, Shephard MS (1984) Automatic three-dimensional mesh generation by the modified-octree technique. *Int J Numer Methods Eng* 20:1965–1990
- Zhao Y, Yang T, Zhang P, Zhou J, Yu Q, Deng W (2017) The analysis of rock damage process based on the microseismic monitoring and numerical simulations. *Tunn Undergr Space Technol* 69:1–17
- Zhou H, Wang C, Han B, Duan Z (2011) A creep constitutive model for salt rock based on fractional derivatives. *Int J Rock Mech Min Sci* 48:116–121
- Zhou J, Yang T, Zhang P, Xu T, Wei J (2017) Formation process and mechanism of seepage channels around grout curtain from microseismic monitoring: a case study of Zhangmatun iron mine, China. *Eng Geol* 226:301–315
- Zhou J, Wei J, Yang T, Zhu W, Li L, Zhang P (2018) Damage analysis of rock mass coupling joints, water and microseismicity. *Tunn Undergr Space Technol* 71:366–381
- Zhu W, Tang C (2004) Micromechanical model for simulating the fracture process of rock. *Rock Mech Rock Eng* 37:25–35

Publisher's Note Springer Nature remains neutral with regard to jurisdictional claims in published maps and institutional affiliations.